RoboSub 2025 Technical Design Report

Shenzhen Technology University (Leviathan Autonomous Systems)

Chengyu Shi, Zhengyang Pei, Yanpei Wang, Qiwen Zheng, Shihan Bao, Xianjie Zhong, Hai Bao, Deguang Ouyang, Shihan Bao, Hanzi Zhang, Shuna Qiu, Niangyue Ye, Haoyang Sun, Hanzi Zhang, Senmiao Zhang,Tao Yang, Chao Wang

Abstract—For RoboSub 2023, the strategy of the sztudragonleap team is to deploy the Leviathan to efficiently complete all tasks.The equipment has been optimised for space, weight and ease of maintenance, and mechanical work has focused on improving the reliability of our manipulators to maximise the success of all tasks.The electrical work is focused on maintaining existing systems and researching new technologies and development processes.Software work has focused on improvements in ease of development and a complete overhaul of the sensory pipework.New components were thoroughly tested in simulation and verified after integration with the vehicle.Introduction

I. COMPETITION STRATEGY

For the 2025 RoboSub competition, we plan to deploy our Leviathan vehicle (Fig. 1) to complete the first four mission tasks. We will focus on optimizing the vehicle's speed and position control specifically for these competition challenges. Through extensive stability testing to validate its capabilities, we strive to achieve a 100% success rate in these tasks. We believe possessing such a robust and stable vehicle will enable us to stand out at this year's RoboSub competition.

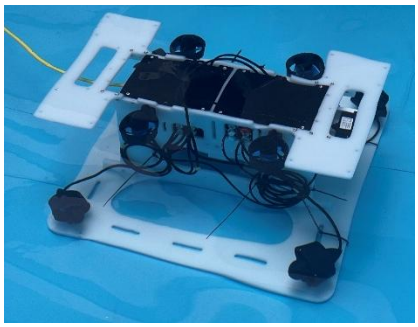

Fig. 1 Vehicle image of Leviathan

A. *Selecting a Template (Heading 2)*

First, confirm that you have the correct template for your paper size. This template has been tailored for output on the US-letter paper size. If you are using A4-sized paper, please close this file and download the file “MSW_A4_format”.

B. *Maintaining the Integrity of the Specifications*

The template is used to format your paper and style the text. All margins, column widths, line spaces, and text fonts are prescribed; please do not alter them. You may note peculiarities. For example, the head margin in this template measures proportionately more than is customary. This measurement and others are deliberate, using specifications that anticipate your paper as one part of the entire proceedings, and not as an independent document. Please do not revise any of the current designations.

II. DESIGN CREATIVITY

A. *Mechanical Sub-System*

1） Design of Main Hull

Constructed from 10mm thick polypropylene (PP) sheet, the main frame utilizes hammerhead nuts and screws for assembly(Fig. 2). It features a three-dimensional, cross-shaped layered structure comprising upper and lower platforms surrounded by side panels. The overall dimensions are 570mm (L) × 540mm (W) × 300mm (H). PP offers excellent resistance to seawater corrosion, eliminating the need for additional surface treatment. Compared to titanium alloy, PP reduces material costs by 60%, and compared to aluminum alloy, it achieves a 28% weight reduction, while maintaining a tensile strength of ⩾35 MPa.

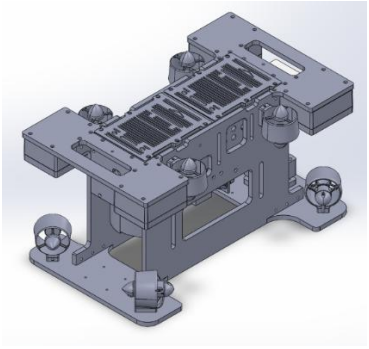

Fig. 2: 3D model of Main Hull

Two aluminum alloy pressure vessels (180mm × 140mm × 1250mm each) are centrally mounted within the frame, stacked laterally. These house the battery pack and the core electronics compartment, respectively. The aluminum alloy, with its high thermal conductivity of 130 W/(m·K), efficiently dissipates heat generated by the circuit boards. Following anodization, the vessels achieve an IP68 waterproof rating, ensuring reliable sealing at depths up to 10 meters. A modular design facilitates rapid component replacement. Each vessel also incorporates its own dismountable features, allowing access for maintenance and troubleshooting without *disassembling the entire frame. This design specifically*

addresses the competition's requirement for "rapid fault diagnosis" under time constraints.

2） Design of Buoyancy leveling

Four buoyancy modules (1L capacity each) are symmetrically mounted at the four corners of the frame, configured as two fore and two aft modules with a lateral spacing of 300mm. Buoyancy trimming is achieved by adjusting the weight within these modules combined with an onboard attitude stabilization algorithm. Each module provides a maximum buoyant force of 1kg, yielding a total adjustable buoyancy range of ±4kg.

3） lDesign of executive device

- Thruster

Four thrusters (3kgf thrust each) are symmetrically mounted on the port and starboard side plates, with 150mm lateral spacing. This configuration enables precise depth control (±0.5m) through coordinated operation, generating 12kg maximum vertical thrust to lift the 5kg payload. Designed with redundancy per IEEE 2024 Underwater Robotics Standards, the system maintains ⩾75% thrust capability during single-thruster failures. The vertical thrusters can counteract vertical currents up to 50cm/s, ensuring stable depth positioning for water quality sensors in stratified environments.

Four bottom-mounted thrusters (5kgf thrust each) are arranged in a rectangular pattern (500mm × 400mm wheelbase) with fore-aft symmetry, implementing quadcopter-inspired control logic. Through Jacobian matrix decoupling, they provide 6-DOF maneuverability including forward/backward motion (1 knot), rotation (15°/s), and lateral translation (0.5 knot), achieving ±10cm positioning accuracy. The thrusters feature hydrodynamically optimized shrouds with 15° inlet diffusers, reducing drag by 12% and preventing bubble adhesion. All eight thrusters are synchronized via PID algorithms, recovering stability within ≤1.2 seconds under 10° roll disturbances - a 40% improvement over conventional quad-thruster systems.

- Launchers

To address the challenge of launch instability, we drew inspiration from the snap structure of a pistol's hammer, designed and tested a launcher that relies on a single plate to resist and store elastic potential energy (Fig .1 (a)), aiming to achieve precise torpedo launch functionality.

We use a servo motor to control the angle rotation, which drives the opening and closing of the launch gate. Closing the launch gate stores sufficient elastic potential energy, and when launching, opening the launch gate allows the torpedo to accurately pass through the opening in the image. During testing, it was found that the fluidity of water would affect the launch stroke. To this end, holes are reserved in the launcher shell to achieve sufficient exchange with the external water flow.

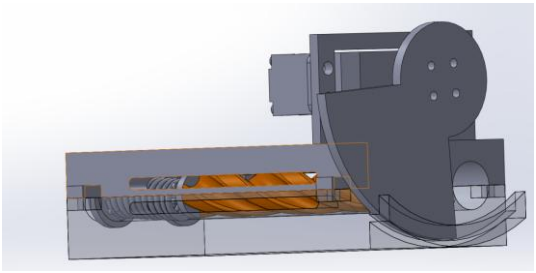

Fig. 3 Structural design of the launcher

The torpedo features a streamlined bullet profile with an ogive-shaped nose and a tapered parabolic tail(Fig. 4). This evolved from an initial prototype that relied on spiral grooves for spin stabilization. Research into underwater projectile dynamics (e.g., Principles of Naval Weapon Systems) confirmed tail fins and helical grooves as primary stabilization methods. Tail fins were eliminated due to 3D-printing fragility, assembly complexity, and minimal trajectory impact (<2% deviation in tests).

- Torpedo

To cope with the impact of water fluidity on the launch stroke, our torpedo design draws on the shape of bullets, adopting a structure with a pointed front and a rounded rear to increase the launch stroke of our torpedo and ensure that it can completely pass through the opening.

The overall structure of our torpedo (Fig.1(b)) maintains a stable state after launch by means of spiral grooves, so as to realize the self-rotation function of the torpedo. A streamlined design is adopted for drag reduction. Considering that the torpedo must meet certain movement performance and stability, we also use a special arc design at the tail of the torpedo, which is designed as a streamlined tail. In addition to reducing drag, it also plays a key role in maintaining the stable state of the torpedo after launch. The design of the torpedo enables reliable long-distance launch, allowing us to meet the challenge of launching the torpedo and accurately and completely passing through the opening in the image.

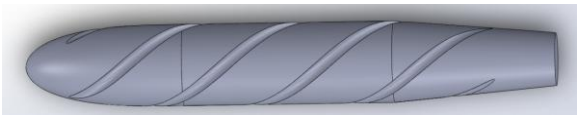

Fig 4. 3D model of torpedo

B. Electrical Sub-System

The Leviathan vehicle implements a star-topology network with the NVIDIA Jetson Nano Orin embedded PC serving as the central hub. Internal communication with the baseboard, PX4 flight controller, and peripheral sensors is established via USB protocol. During mission debugging, a standard Ethernet cable provides the external communication link between the onboard computer and the ground station.

1） Communication Architecture

The Leviathan vehicle implements a star-topology network with the NVIDIA Jetson Nano Orin embedded PC serving as the central hub. Internal communication with the baseboard, PX4 flight controller, and peripheral sensors is established via USB protocol. During mission debugging, a standard Ethernet cable provides the external communication link between the onboard computer and the ground station. Communication link between the onboard computer and the ground station.

2） Power Architecture

The baseboard (Fig. 5) integrates comprehensive functionality including auxiliary power conversion with multi-rail regulated outputs: 24V@10A, 12V@5A, 7.4V@5A, 5V@5A, and 3.3V@3A. All interfaces incorporate triple-layer protection: reverse-polarity protection, short-circuit protection, and TVS-based transient surge suppression. The board additionally features hot-swappable capability for field maintenance operations.

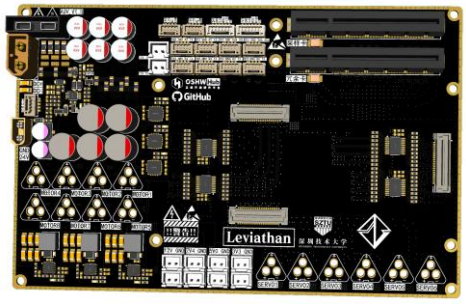

Fig. 5 3D model of baseboard

3） Sensor Architecture

The primary sensors comprise an Inertial Measurement Unit (IMU) for attitude detection, a depth sensor for depth measurement, a hydrophone array for underwater heading determination, and two cameras. For attitude detection, we employed a 9-axis IMU integrated with geomagnetic field detection, coupled with a sensor fusion drift correction algorithm to mitigate inherent sensor drift. The depth sensor utilizes a strain-gauge pressure transducer to measure hydrostatic pressure for determining water depth. The underwater navigation system incorporates a multibeam sonar and sampling system for determining underwater heading. For vision, a binocular stereo camera was adopted to acquire sub-pixel visual features for model training.

4） Actuator Architecture

The actuation system consists primarily of underwater thrusters for propulsion and servo-based actuator assemblies for task execution. The thrusters employ brushless AC motors housed within corrosion-resistant enclosures (marine-grade aluminum alloy). An eight-thruster configuration enables full six-degree-of-freedom maneuverability, providing enhanced acceleration capability during vertical transit. For mission-specific actuation, waterproof servomotors with corrosion-resistant housings serve as the primary actuation source for task-oriented mechanisms.

III. SOFTWARE SUB-SYSTEM

After the text edit has been completed, the paper is ready for the template. Duplicate the template file by using the Save As command, and use the naming convention prescribed by your conference for the name of your paper. In this newly created file, highlight all of the contents and import your prepared text file. You are now ready to style your paper; use the scroll down window on the left of the MS Word Formatting toolbar.

A. Controller systems

To address the high performance control requirements of the robot for the competition, we selected the PX4 control system as our attitude controller.The PX4 flight controller estimates the attitude (heading, pitch, roll) and motion state of the AUV by reading data from sensors such as IMU, magnetometer, underwater manometer, etc. and executes the control algorithms in accordance with the preset goals.The flight control firmware usually adopts a sensor fusion module docs.px4.io based on Extended Kalman Filtering (EKF).We fuse the fused inertial, magnetic field, and depth information, and output state estimates including attitude quaternion, velocity, and position docs.px4.io, which are used as inputs into the control loop to improve control accuracy and robustness.

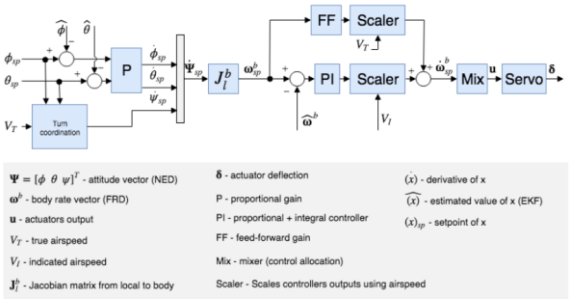

Figure 1Self-stabilising algorithm diagram

Our attitude control uses a typical cascade PID structure.The inner loop is an angular velocity control loop (Rate Controller) that uses a proportional-integral (PI) controller to fast track angular velocity commands, and the outer loop is an attitude-angle control loop (Attitude Controller) that uses a proportional (P) controller to convert attitude commands to angular velocity targets.P The flight control rotates parametrically in quaternionic numbers to improve the numerical stability of the attitude control.The P flight control is parametrically rotated in quaternions to enhance the numerical stability of attitude control.In addition, the Angular Velocity Controller filters the gyroscope signals and provides anti-saturation processing for the integration loop to ensure that the system response is both fast and smooth.

B. PC core software system

The onboard computing subsystem, powered by NVIDIA Jetson Nano, hosts the high-level intelligence layer of the AUV. A Robot Operating System 2 (ROS 2)-based modular software framework is deployed on Jetson, organizing the entire mission execution stack into distributed nodes. Each

node serves a dedicated function, such as sensor acquisition, object detection, trajectory planning, or data logging. These nodes communicate via the ROS 2 publish/subscribe messaging system, supporting parallelism and modularity.

Figure 2jetson nano core board

To meet the demands of real-time underwater operation, Jetson Nano employs multi-threaded executors provided by ROS 2. These allow concurrent callback processing across nodes, thus leveraging the four-core ARM CPU and integrated GPU. This architecture ensures that latency-sensitive modules, such as perception and control, receive adequate processing bandwidth.

The perception pipeline typically incorporates camera nodes alongside deep learning inference engines. Ultralytics YOLO or the Jetson-inference framework is utilized to perform real-time object detection accelerated by CUDA. The visual data undergo pre-processing (e.g., denoising, contrast adjustment) using OpenCV, followed by neural inference to identify and classify objects. The resulting information, such as object position and class, is published to downstream planning or tracking nodes.

IV. TEST STRATEGY

A. *Power supply test*

A dedicated inrush current control circuit was designed for the vehicle power system, encompassing both the 24V power rail for the high-power domain and auxiliary power rails for other subsystems. Furthermore, a controlled power-up sequence is implemented, wherein the controller circuitry is energized first, followed by the stabilization of the high-power domain supply. This sequencing enhances system reliability. The corresponding test configuration is depicted in Fig. 6.

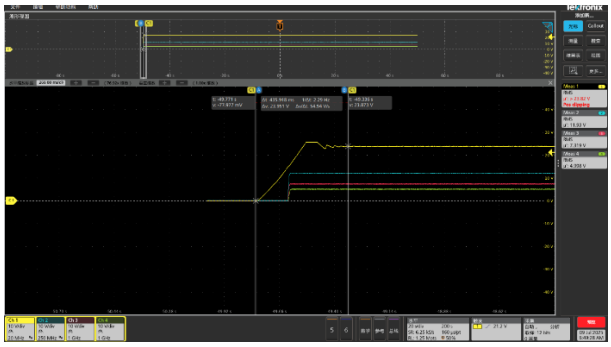

Power-up sequence waveform capture

B. *Propulsion testing*

The vehicle's thrusters are governed by the PX4 flight controller board. During installation verification, we conducted validation using the QGroundControl (QGC) software suite - the official ground station companion for PX4 systems (Fig. 7).

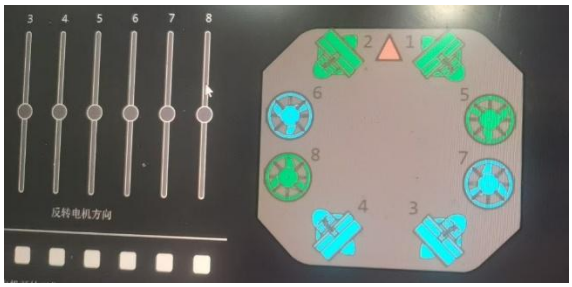

QGC Thruster Validation Protocol

REFERENCES

[1] T. Wu, Y. Xu, Y. Li, and J. Wang, “Fault-tolerant control for AUVs using a single thruster,” IEEE Access, vol. 10, pp. 40099–40111, 2022, doi: 10.1109/ACCESS.2022.3166331.

[2] L. Xu, Y. Xu, C. Lin, and Y. Wang, “Layout and geometry optimization design for 3D printing of self-supporting structures,” Data in Brief, vol. 50, p. 109349, 2023, doi: 10.1016/j.dib.2023.109349.

[3] S. H. Kim, Y. S. Oh, and H. J. Kim, “Design of a finless torpedo shaped micro AUV with high maneuverability,” in Proc. IEEE Underwater Technology (UT), Busan, 2017, pp. 1–5, doi: 10.1109/UT.2017.8232083.

[4] Y. Tan, Z. Du, Y. Ren, and S. Liu, “Parameterization and optimization for the axisymmetric forebody of hypersonic vehicle,” Ocean Engineering, vol. 190, p. 106418, 2020, doi: 10.1016/j.oceaneng.2019.106418.

[5] A. E. Elsayed, A. A. Khalaf, M. A. Elshaer, and Y. A. Khalil, “Long-term performance of interlayer hybrid composites of polypropylene and glass fiber exposed to salt solution and deionized water at elevated temperatures,” Construction and Building Materials, vol. 420, p. 136083, 2024, doi: 10.1016/j.conbuildmat.2024.136083.

[6] R. Martins, J. Almeida, and A. Matos, “Modular building blocks for the development of AUVs — from MARES to TriMARES,” in Proc. IEEE OCEANS, Bergen, 2013, pp. 1–9, doi: 10.1109/OCEANS-Bergen.2013.6519897.

[7] Y. Zhang, J. Zhang, and H. Li, “Design and hydrodynamic analysis of subsea development automatic placement devices,” Frontiers in Mechanical Engineering, vol. 11, p. 1562920, 2025, doi: 10.3389/fmech.2025.1562920

APPENDIX A TORPEDO ANALYSIS

- Torpedo:

The torpedo design draws inspiration from bullet ballistics, featuring a pointed nose and rounded tail. The initial torpedo nose curve was relatively arbitrary, and helical grooves were machined to induce spin and maintain post-launch stability.

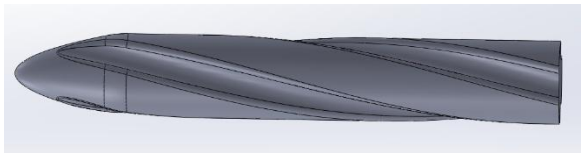

Figure: The first generation of torpedo design

Research identified two primary methods for stabilizing torpedoes: adding fins or machining helical grooves.

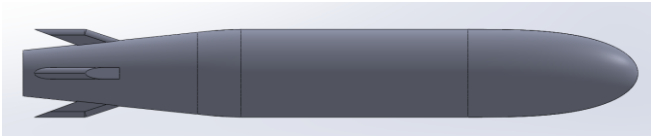

Figure: The second generation torpedo design

However, fin attachment proved problematic due to printing difficulties, extreme fragility, and minimal observed impact on launch performance in tests. Consequently, a finless torpedo design was finalized. To minimize hydrodynamic drag during travel, special streamline profile curves were designed for both the nose and tail sections, generated by rotating these curves around the central axis.

Streamlining Drag Reduction Principle: In fluid dynamics, a streamlined shape effectively reduces drag by guiding fluid flow smoothly over the object's surface. This minimizes flow separation and vortex formation, which create low-pressure zones and energy loss. The designed curves apply this principle, enabling water to flow more smoothly over the torpedo surface, lowering the drag coefficient, reducing energy loss, and thereby enhancing speed and efficiency.

Formula Parameter Significance: For the nose curve formula $y = 7.7 \times (1 - (\frac{x}{30})^3)^{\frac{1}{2}}$, the parameters 7.7 and 30 were determined based on the torpedo's actual dimensions and design requirements. The value 30 represents a characteristic length of this nose section, while 7.7 is a scaling coefficient related to the nose shape. The exponents 3 and $\frac{1}{2}$ create the specific tapering point profile essential for streamlining and reducing impact drag at the head.

Tail Curve Impact on Stability: Beyond drag reduction, the tail's special curve design crucially contributes to maintaining post-launch stability. The streamlined tail promotes smooth flow detachment, reducing wake turbulence and consequent torpedo yaw or wobble.

Parameter Explanation: Similarly, for the tail curve formula $y = 7.5 \times (1 - (\frac{x}{30}))$, parameters like 7.5 and 30 control the tapering rate and shape based on design needs. The exponent of 1 results in a gentler curve, effectively reducing wake vortices and drag. This mathematically controlled shape ensures a smooth transition and gradual taper, minimizing flow separation and vortex generation to improve motion performance and stability.

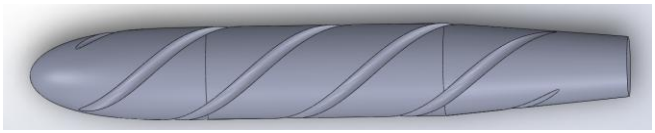

Figure: Final Torpedo Design

- Marker Dropper

Steel balls were selected as the marker payload due to their high density, which minimizes deviation during descent. The mechanism operates via a servo motor driving a blocking plate through a fixed angle of rotation, enabling marker release. When designing the dropper housing, sufficient openings were incorporated into the shell to mitigate buoyancy fluctuations affecting the robot during submersion.

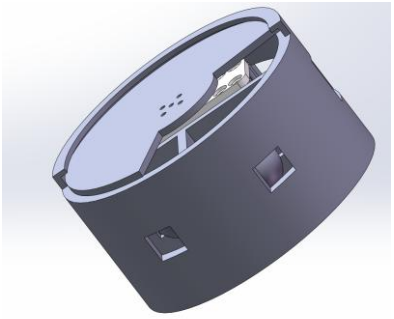

Figure: Marker Dropper Assembly

APPENDIX B The whole machine hardware and software design diagram

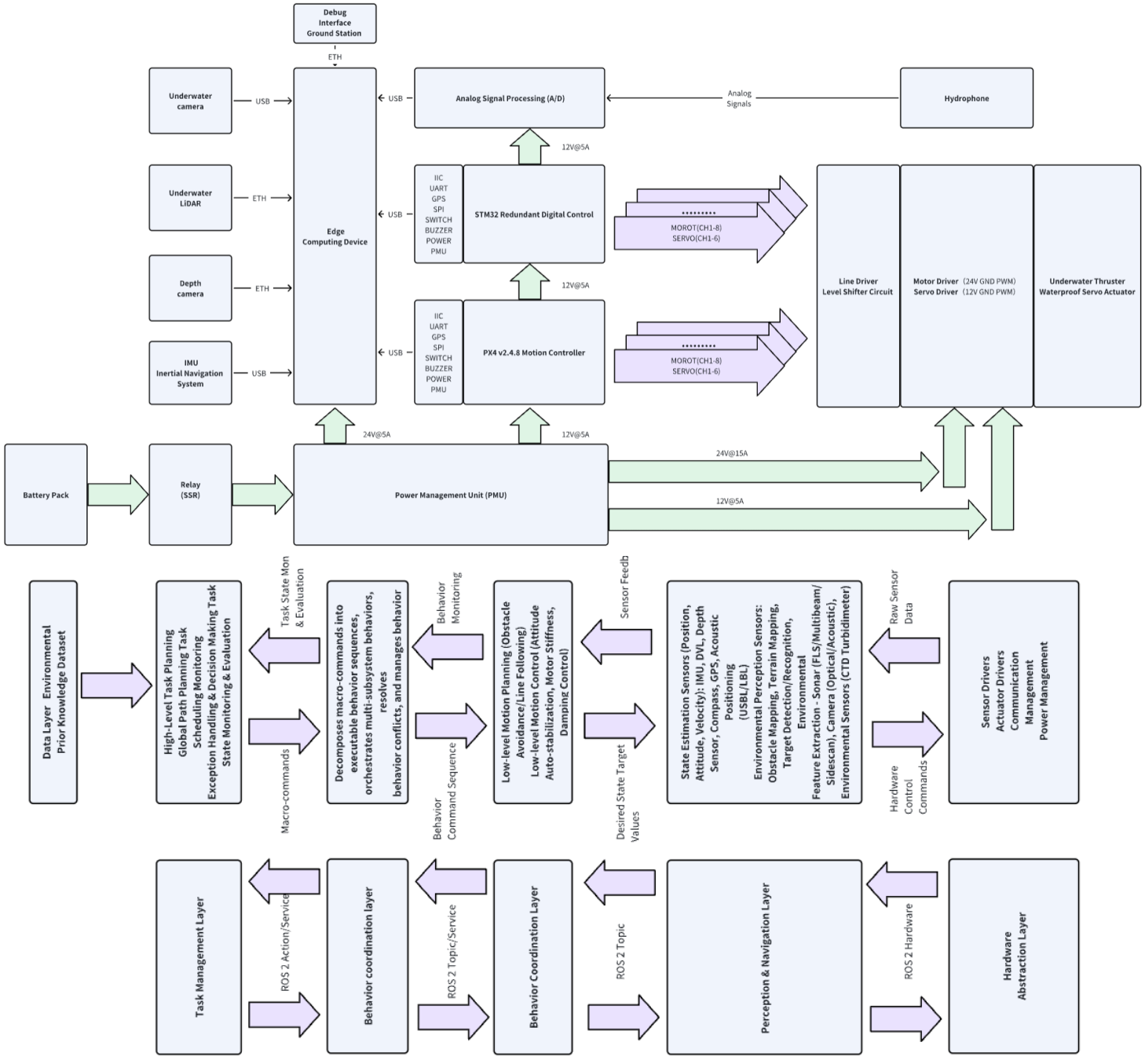

APPENDIX C
COMPONENTSPECIFICATIONS

Component	Vendor	Model /Type	Specifications	Custom /Purchased	Cost	Year of Purchase
Frame Structure	Quanzhou Smart Manufacturing	—	—	Custom	$100	2025
Waterproof Housing	Quanzhou Smart Manufacturing	—	—	Custom	$200	2025
Thruster Assembly	Pacific Technologies	P75（1）	24V	Purchased	$14.1	2025
Motor Controlle	Pacific Technologies	P75（2）	24V	Purchased	$42.7	2025
Main Control Unit	Quansheng Electronics	Pixhawk 2.4.8	—	Purchased	$72	2025
Propeller	Pacific Technologies	P75（3）	24V	Purchased	$2	2025
Battery Pack	Suoqi	—	24V 12000mAh (4P6S Configuration)	Purchased	$37	2025
Central Processing Unit	AeroMech Innovations	Jetson Orin NX Super	16GB	Purchased	$850	2025
IMU	YABO Intelligenc	N200	10-DOF	Purchased	$20	2025
Acoustic Equipmen	SynAcoustic Micro-Detectio	W-025	—	Purchased	$1000	2025

APPENDIX D
SPONSORS

A. Title Sponsors
SZTU would like to thank Shenzhen University of Technology (SZTU) for providing financial and technical support as well as the patience of the relevant teachers.

B. Platinum Sponsors
Qingdao CeHai Automation Technologies Co., Ltd.
Thanks to Qingdao CeHai Automation Technologies Co., Ltd. for providing relevant technical guidance